Ocean Engineering 154 (2018) 106–120

Contents lists available at ScienceDirect

Ocean Engineering

journal homepage: www.elsevier.com/locate/oceaneng

# AUV homing and docking for remote operations

N. Palomeras *, G. Vallicrosa, A. Mallios, J. Bosch, E. Vidal, N. Hurtos, M. Carreras, P. Ridao

*Underwater Robotics Research Center (CIRS), Computer Vision and Robotics Institute (VICOROB), Universitat de Girona, 17004 Girona, Spain*

ARTICLE INFO

*Keywords:*
AUV
Docking station
Acoustic localization
Visual tracking
Remote operation

ABSTRACT

One of the major goals of the SUNRISE FP7 project is to make the Underwater Internet of Things a reality. In this context, the LOON-DOCK project presented here extends the existing Litoral Ocean Observatory Network testbed with a Docking Station tailored to the Sparus II AUV. The docking system allows a remote user to program survey-like missions through a web-based interface as well as to retrieve the data gathered by the AUV once a mission finalizes. To enable the autonomous docking of the AUV, two complementary and cost-effective localization systems have been developed. The first one implements a range-only localization algorithm to approach the docking station while the second, based on active light beacons, provides high accuracy at short ranges to complete the docking maneuver. The system has been extensively tested, in different trials from a controlled water tank environment to more realistic sea operation conditions proving its viability despite very poor water visibility conditions.

## 1. Introduction

The increased number of deployed subsea systems (infrastructures, sensors, robots, gliders and others) during the last years, is raising the need for interconnection among themselves and to the exterior world, for a better management and exploitation. This is one of the major goals of the SUNRISE FP7 project (Petrioli et al., 2013), which is devoted to make the Underwater Internet of Things (UIoT) a reality. Connecting the underwater systems to the network and endowing them with the capability of making their data widely accessible while minimizing the need of human interaction, has the potential of providing ocean data at an unprecedented scale.

Persistent deployment of buoyancy-driven vehicles (gliders) in open waters has already been achieved for periods of time spanning months (Manley and Willcox, 2010; Meyer, 2016). However, persistent deployment of survey-type Autonomous Underwater Vehicles (AUVs), capable of more complex mapping missions, is a challenging problem that arises the requirement of docking. The objective behind the docking concept is to extend the deployment time by installing a Docking Station (DS) that allows to extract the data of finished missions, program new missions and recharge the batteries of the vehicle without recovering it at the surface. The first systems were designed for oceanographic sampling purposes (Curtin et al., 1993; Singh et al., 2001). More recently, the interest has grown towards using AUVs in commercial scenarios, for the periodic inspection and maintenance of subsea installations (Brignone et al., 2007; Krupinski et al., 2008; Jacobson et al., 2013). In addition, a significant part of docking-related works have emerged from operational environments where launch and recovery is a difficult task such as under ice operations (King et al., 2009). However, despite many demonstrations have taken place since the 90's, the combined need of infrastructure (physical mounting, power, communications) and the demanding vehicle reliability required to operate continuously without human servicing, still makes docking a state-of-the-art problem (Bellingham, 2016).

In the context of the SUNRISE project, the LOON-DOCK project presented here aims to extend the existing Litoral Ocean Observatory Network (LOON) testbed (Alves et al., 2014) with a DS to demonstrate data transmission from a survey-AUV to the Internet. The idea is to be able to remotely operate the AUV from the SUNRISE GATE, (Petrioli et al., 2014), a web interface created to remotely schedule experiments using assets persistently deployed in different testbed facilities around the world. For the AUVs to really become part of the UIoT, it is essential to provide docking solutions that are cost-effective, while maintaining the performance and reliability of the system. In this sense, our proposal strives to keep the implemented docking approach low-cost in all the addressed aspects, namely the mechanical design, the communications and the autonomous docking procedure. The power transference to the AUV is not covered in the scope of this work. However, it is worth noting that solutions for wireless inductive power transference already exist in the market and could be integrated at a certain cost.

From the hardware point of view, the developed DS is based on a

* Corresponding author.
*E-mail address:* npalomer@eia.udg.edu (N. Palomeras).

https://doi.org/10.1016/j.oceaneng.2018.01.114
Received 8 May 2017; Received in revised form 21 November 2017; Accepted 31 January 2018
Available online 12 February 2018

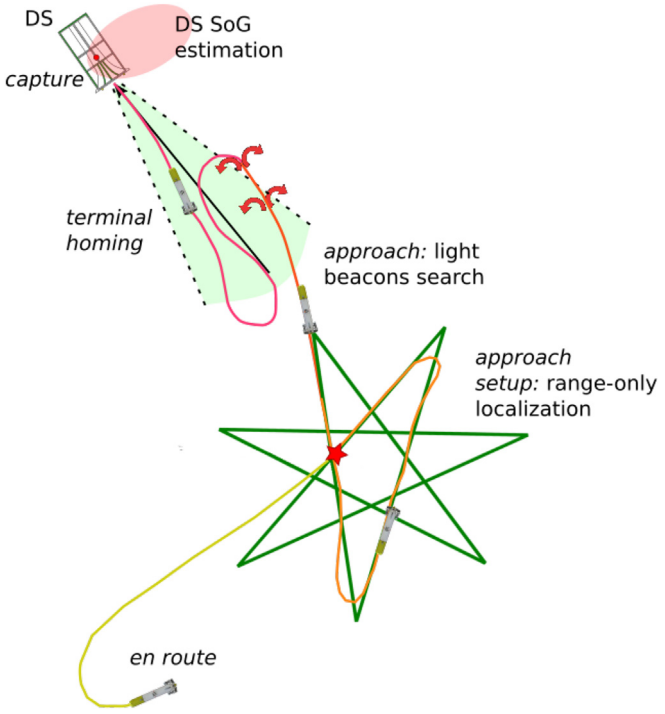


**Fig. 1.** Docking phases scheme.

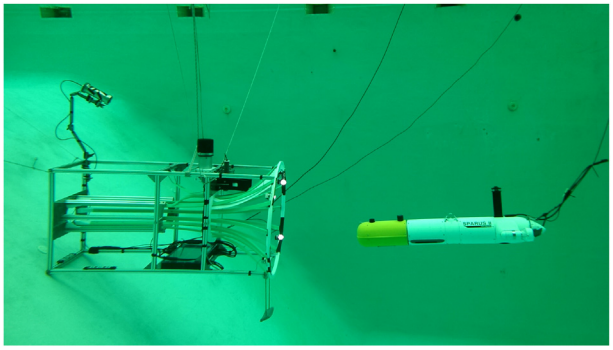

**Fig. 2.** Testing the docking station and the approach procedures in a water tank. The AUV cable visible in the image is only for monitoring purposes.

funnel-shaped receptacle, which is a traditional solution (Cowen et al., 1997; Allen et al., 2006; McEwen et al., 2008) to physically guide the vehicle into the dock. Another common design found in the literature are the vertical dock poles (Singh et al., 2001; Stone et al., 2010) that allow the vehicle to approach from any direction, making them more robust to changing water disturbances. To alleviate the directionality constrain, the funnel receptacle has been designed so that it can pivot over the static base and be oriented according to the water currents of the environment. Compared to a pole dock, the funnel-shaped design eases the installation of the necessary equipment to support the communications and the homing maneuvers, facilitates the establishment of links with the vehicle and protects the AUV against environmental hazards while docked. With regards to communications, the developed docking system is directly connected to the Internet through the LOON infrastructure, and features two modes of communication with the AUV. The first mode uses an acoustic modem and the SUNSET protocol (Petrioli et al., 2015), a lightweight networking framework well-suited for underwater acoustic communications. The second mode, intended for when the AUV is docked, is based on a contactless WiFi module installed in the DS, which is crucial to transfer at high speed the vast amounts of data that a survey-AUV can gather in a mission. The use of a contactless radio frequency module, based on a commercial off-the-shelf (COTS) WiFi modem, provides a reliable and low-cost data transmission system (McEwen et al., 2008) capable of achieving transfer speeds in the order of tens of Mbps. It does not require the mating of connectors underwater, thus preventing the exposure of electrical contacts, and provides a less sensitive alignment with respect to establishing direct electrical connections (Stokey et al., 2001) or inductive coupling (Feezor et al., 2001).

To assist the autonomous docking procedure, the DS employs the acoustic modem as a range-only transponder for mid-range homing, and a set of light beacons installed in the funnel entrance for the terminal phase of the docking. The autonomous docking is tackled from the general scenario in which the vehicle does not know the exact position of the DS, usually because it has lost the communication with the DS during a mission execution and only has an *a priori* coarse estimate of its position. Then, following the nomenclature established in Bellingham (2016), our proposed approach for autonomous docking works as follows (see Fig. 1): first, the vehicle starts from an *en route* phase, that gets the vehicle close enough so it can sense the DS with the on-board acoustic transponder. This navigation is performed according to the on-board navigation filter that merges information from different sensors to navigate relative to the Earth. Next, in the *approach-setup* phase, a range-only localization filter is used to estimate the DS location while the AUV is guided along an observable trajectory. Once an estimation of the DS position becomes known, the vehicle approaches the DS to bring it within visual reach (i.e., *approach* phase). The light beacon navigation system is used to estimate the DS pose with respect to the AUV on-board camera. Visual information is used to update a single landmark simultaneous localization and mapping filter that provides the relative position between the AUV and the DS with the accuracy required for the *terminal homing* phase. Preliminary versions of these two localization algorithms have been previously reported in a simulation environment (Vallicrosa et al., 2016). In order to back up the visual localization during the very last few meters of the approach, when the light beacons are no longer inside the camera field of view, a complementary system has been integrated using augmented reality (AR) markers (Garrido-Jurado et al., 2014). After this phase, the AUV ends up inside the docking funnel and is guided up to the latch mechanism by controlling the generated forward thrust (i.e., *capture* phase).

Existing solutions to perform autonomous docking usually rely in more complex acoustic sensors including USBL (McEwen et al., 2008; Allen et al., 2006) or inverted SBL setups (Smith and Kronen, 1997). Optical sensors have also been explored for the terminal phase, with solutions comprising either active light sources -with single (Cowen et al., 1997; Murarka et al., 2009; Li et al., 2015, 2016) or multi-light systems (Hong et al., 2003; Park et al., 2009)- or passive patterns and markers (Kushnerik et al., 2009; Maire et al., 2009) that can be detected by on-board cameras. Altogether, our approach provides an hierarchical homing procedure that ensures a reliable approach and terminal homing maneuvers enabled with low-cost equipment and minimal requirements on both the vehicle and the DS sides. Notice that, indeed, the acoustic ranging and optical image acquisition are capabilities that either already exist in most AUVs or can be easily added at a reasonable cost. The same reasoning applies to the docking station, since the light beacon system and the AR markers are relatively inexpensive to manufacture.

The reminder of this paper is organized as follows: next section describes in more detail the employed AUV and the design of the proposed docking station. Section 3 introduces the navigation system of the AUV together with the developed algorithms for autonomous docking, including both the range-only localization and the visual localization of the DS. Section 4 covers the insights about operation and control, involving the remote operation through the SUNRISE web-based

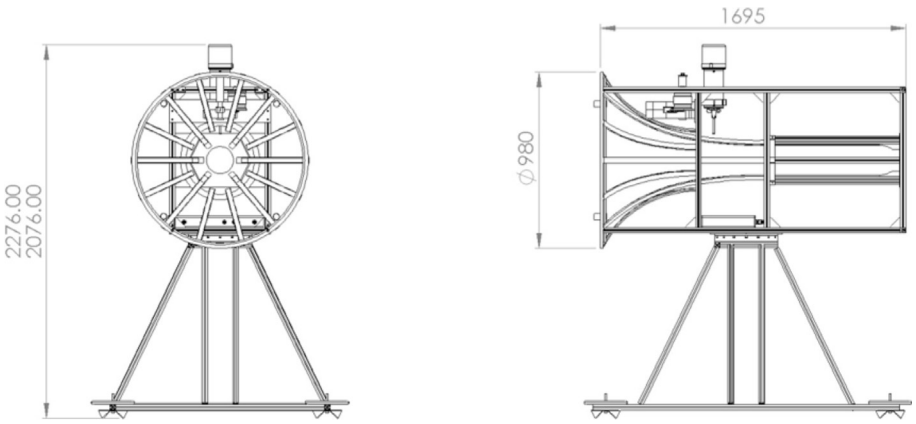


**Fig. 3.** Docking station CAD model (dimensions in mm).

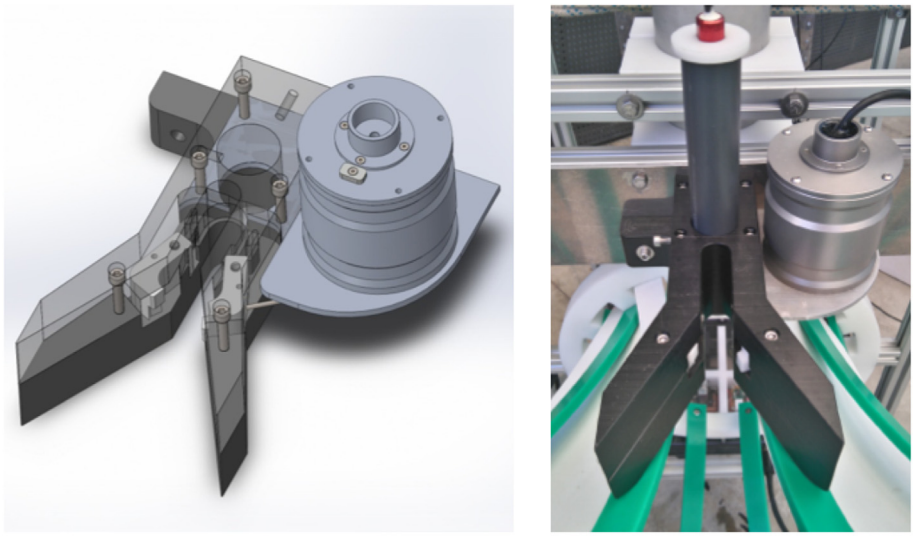


**Fig. 4.** (a) CAD model of the latching mechanism and (b) picture of the real latching mechanism.

interface and the AUV guidance module that controls the various phases of the autonomous docking. Section 5 presents the experiments that have been performed together with an analysis of the results obtained with the system fully integrated in the LOON infrastructure. Finally, Section 6 reports the conclusions and points out future work directions.

## 2. Hardware

The DS has been designed especially for the Sparus II AUV (Carreras et al., 2013) (see Fig. 2). Sparus II AUV is a lightweight (i.e., 50 kg) torpedo-shaped vehicle with partial hovering capabilities. It has two horizontal and one vertical thrusters, allowing surge, heave and yaw movements, and a mission-specific payload area. Its flexibility and easy operation makes the Sparus II AUV a multipurpose platform adaptable to a high variety of mapping applications in shallow water (i.e., up to 200 m).

The DS provides active and passive guidance for docking, a latching mechanism to maintain the vehicle docked while in standby mode, high bandwidth data communications, and visual feedback.

The DS has been designed to be as small as possible and lightweight for easy transportation, deployment, and recovery. It is constructed mainly from corrosion resistance aluminium and polyoxymethylene (POM). The structure consists of two main parts, the docking part and the base (see Fig. 3). The entrance of the docking part has fourteen funnel-shaped rails that passively guide the vehicle to the dock position using vehicle's thrust. The size of the funnel can handle translation misalignment of 40 cm and rails arrangement can correct vehicle misalignment's in roll and pitch up to 30deg. Rail guides are made from flexible POM which can absorb collisions, thus minimizing vehicle back bouncing.

The base connects with the docking part with a single axis rotation mechanism that allows the docking part to align with water currents without moving the base. Current implementation requires manual input for the rotation (i.e., by using a diver), however, in the future an active automatic mechanism will be implemented. The base feet can be adjusted up to 20 cm in height in order to level the DS and accommodate ballast weights to keep the centre of gravity low.

A latching system (see Fig. 4) has been developed to prevent the vehicle from exiting the DS due to water currents thus allowing it to enter in low power mode once docked. When the vehicle has entered the DS in its final position, two claws grip on the antenna does not allow the AUV to exit. The operation of the claws is controlled from a servo motor. There is a solid join between the motor and the right claw and from this the motion is propagated to the left claw via flexible wires. The servo motor, when activated, has enough torque to withstand opening forces if the

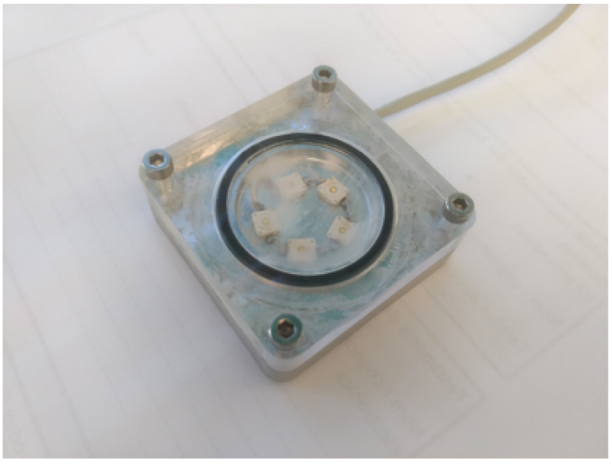

**Fig. 5.** Light beacon hardware design.

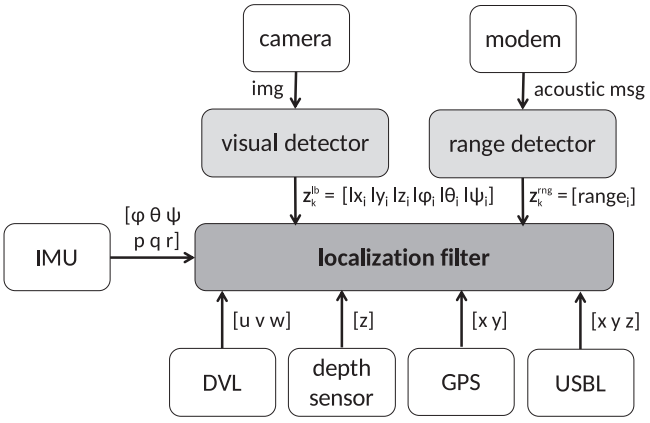


**Fig. 6.** Set of sensors that take part in the navigation algorithm of the AUV software architecture.

vehicle tries to exit due to water currents or even with its thrusters. However, if it is deactivated, such in the event of a DS power loss, the claws are disengaged and with relatively small thrust the AUV can safely exit.

Two active systems provide mid and short range localization information to the AUV in order to guide it to the DS using the algorithms that will be described in Section 3.

For mid range detection, an Evologics acoustic modem is installed on the top of the DS, performing two main functions: a transponder function providing range measurements for homing and a modem function to monitor the AUV during survey operations and to allow the user to send basic commands to the AUV remotely.

For short range guidance, when the DS is within the AUV visual range of its camera, light beacons are used to provide localization aid. There are four beacons installed around the entrance ring in a symmetrical fashion.

Each individual light beacon consists of five high-intensity LEDs to create a homogeneous lighting effect inside a waterproof housing (see Fig. 5). Each beacon provides flashing light at approximately 110deg field of view (FoV)FOV at 1 Hz period with 90% on - 10% off duty cycle. The system is operated at 24 V, and the maximum power consumption is 22 W, when all markers are lit. The beacons can be remotely activated from top-side.

Two high-bandwidth data communications interfaces have been included in the DS: one between the top-side and the DS, and one between the DS and the AUV.

It is very common to install the DS in long distance from the top-side base. Establishing communications between them can be achieved either by wireless connection via a surface buoy or by fixed wire. Given that in the area where the system was demonstrated (i.e., the LOON testbed) there are restrictions for installing permanent surface buoys, we chose to implement a wired connection with a long cable laying on the seafloor. Nevertheless, the DS can be easily modified to support wireless connection.

For the wired communication scheme we are using VDSL2 technology. It supports, via a single twisted pair, up to 100Mbit/s downstream rates at 500 m and graduate decreasing to 1-4Mbit/s over distances of 4–5 km. We have also included an Ethernet connection, though it can only be reliably used for distances shorter than 100 m.

For the AUV to DS communication a WiFi modem has been adapted to fit in a waterproof housing and is positioned on the latching mechanism. When the AUV is docked, its WiFi antenna is close enough to the modem ($\approx$ 7 cm) to allow a strong wireless data link. With this system we are able to communicate with up to 45Mbit/s between the AUV and the top-side.

On the DS there is a watertight container that houses all the necessary electronic components for its operation. That includes a pressure sensor, an inertial measurement unit (IMU) and an Ethernet switch connecting the Evologics modem, the WiFi modem, and a Raspberry Pi 3 single board computer. The Raspberry Pi 3 is locally running ROS (Quigley et al., 2009) and provides control for the latch mechanism and the LEDs. It is also in charge to broadcast through the modem the DS depth and orientations, obtained from the IMU, in order to check that the DS has been properly leveled during its installation. Besides, there is also a webcam that points to the center of DS imaging the AUV when it is docked. There is also an independent underwater analog video camera that is placed on the side of the DS, providing a general overview of the DS and the AUV when approaching.

The DS is connected to top-side via two independent cables, one for power and one for data, to minimize electromagnetic interferences. It is powered with 220VAC via an isolation transformer in order to minimize power loss. The data cable is an Ethernet CAT 5e cable, where one pair is used for the VDSL2, one for the analog video, and the last four are used for the short range Ethernet link.

## 3. AUV navigation and DS localization

The navigation filter of the Sparus II AUV is based on the well known extended Kalman filter (EKF). It combines the information on depth returned by the pressure sensor, velocities from the Doppler velocity log (DVL) and attitude from the attitude and heading reference system (AHRS) to provide a dead reckoning (DR) navigation. This navigation drifts over time and needs absolute measurements to correct it. Those measurements can come from either global positioning system (GPS) when on surface, ultra-short base-line (USBL), or acoustic ranges or visual detections with respect to a known landmark (see Fig. 6).

A feature-based EKF-SLAM navigation filter is used in the proposed scenario where the only landmark will be the DS. The state vector for the implemented filter is the following:

$$\boldsymbol{x} = [x \quad y \quad z \quad u \quad v \quad w \quad \boldsymbol{l}_1 \quad \dots \quad \boldsymbol{l}_N], \tag{1}$$

where $[x\ y\ z]$ and $[u\ v\ w]$ are the position and linear velocity vectors of the AUV, and $\boldsymbol{l}_i$ is the landmark $i$ pose vector defined as:

$$\boldsymbol{l}_i = [lx_i \quad ly_i \quad lz_i \quad l\phi_i \quad l\theta_i \quad l\psi_i]. \tag{2}$$

Because range-only measurements cannot estimate the landmark orientation, a landmark must be initialized by a visual detection. However, once in the state vector, both range-only and visual-based updates can be applied.

The navigation filter uses a constant velocity model with attitude input:

$$\boldsymbol{z}_k^{rng} = \left[\sqrt{rng^2 - (z_V - z_{DS})^2}\right]$$

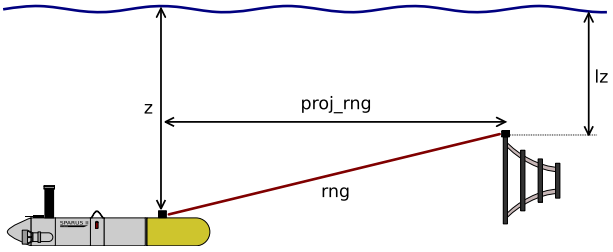


**Fig. 7.** Projection of the range measurement.

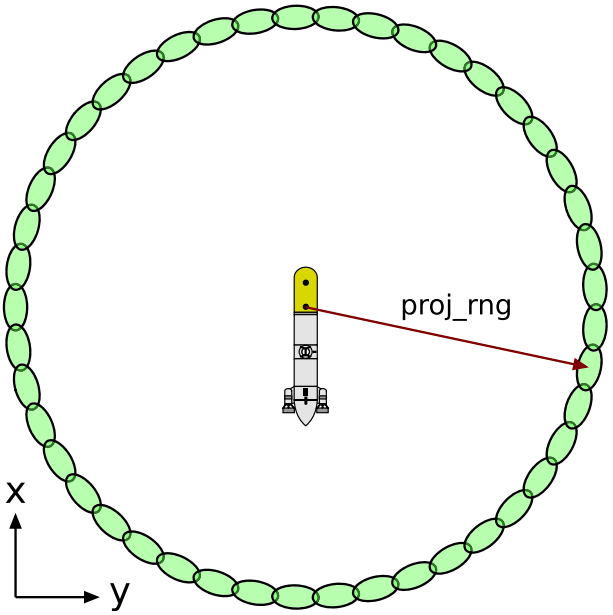


**Fig. 8.** Initialization of the SOG filter ($2\sigma$ bounds).

$$\widehat{\boldsymbol{x}}_k = \begin{bmatrix} \begin{bmatrix} x_{k-1} \\ y_{k-1} \\ z_{k-1} \end{bmatrix} + \mathscr{R}(\phi_k\theta_k\psi_k)\left(\begin{bmatrix} u_{k-1} \\ v_{k-1} \\ w_{k-1} \end{bmatrix} t + \begin{bmatrix} n_{u_{k-1}} \\ n_{v_{k-1}} \\ n_{w_{k-1}} \end{bmatrix} \frac{t^2}{2}\right) \\ u_{k-1} + n_{u_{k-1}} \\ v_{k-1} + n_{v_{k-1}} \\ w_{k-1} + n_{w_{k-1}} \\ l_{1_{k-1}} \\ \dots \\ l_{N_{k-1}} \end{bmatrix}, \tag{3}$$

where $t$ is the sample time, $[n_u\ n_v\ n_w]$ is the noise vector and $[\phi_k\ \theta_k\ \psi_k]$ are the Euler angles used as the filter input $\boldsymbol{u}_k$. Each sensor measurement is modelled as:

$$\boldsymbol{z}_k = H\widehat{\boldsymbol{x}}_k + \boldsymbol{s}_k, \tag{4}$$

where $\boldsymbol{z}_k$ is the measurement itself, $H$ is the observation matrix that relates the state vector with the sensor measurement ($h(\widehat{\boldsymbol{x}}_k)$ if the measurement is not linear), and $\boldsymbol{s}_k$ is the sensor noise. To differentiate between range and light beacon measurements we will use $\boldsymbol{z}_k^{rng}$, $h^{rng}()$ and $\boldsymbol{z}_k^{lb}$, $H^{lb}$ respectively.

In case of range-only measurements, the observation equation provides the expected range measurement $h^{rng}(\widehat{\boldsymbol{x}}_k)$ which is given by the norm of the difference between the vehicle and beacon positions at time $k$.

$$h^{rng}(\widehat{\boldsymbol{x}}_k) = ||(x, y, z) - (lx_i, ly_i, lz_i)||. \tag{5}$$

In the case of a visual detection measurements, updates are linear being

$$\boldsymbol{z}_k^{lb} = [lx_i\ ly_i\ lz_i\ l\phi_i\ l\theta_i\ l\psi_i], \tag{6}$$

and

$$H^{lb} = \begin{bmatrix} -\mathscr{R}(\phi_k\theta_k\psi_k)^T & 0_{3\times3} & \mathscr{R}(\phi_k\theta_k\psi_k)^T & 0_{3\times3} & \dots \\ 0_{3\times3} & 0_{3\times3} & 0_{3\times3} & I_{3\times3} & \dots \end{bmatrix}, \tag{7}$$

where $[lx_i\ ly_i\ lz_i]$ is the relative position of the landmark with respect to the vehicle, $[l\phi_i\ l\theta_i\ l\psi_i]$ is the landmark orientation with respect the inertial frame and $\mathscr{R}(\phi_k\theta_k\psi_k)$ is the vehicle orientation rotation matrix at time $k$.

When the position of the DS is unknown or known with a high uncertainty, the range-only localization method described in Section 3.1 is used to obtain an approximate location. Once the vehicle homes to the vicinity of the DS, the light beacon detection system will be used to initialize the landmark in the EKF-SLAM navigation filter and to provide accurate updates (see Section 3.2).

### 3.1. DS range-only localization

Range-only localization is a highly non-linear problem. Given 1D measurements (range), the vehicle must be localized in a higher dimensional space (3D). With an unknown position of the beacon and after the first measurement, the probability distribution has the shape of a spherical shell with thickness equal to the range measurement uncertainty. Kalman filter (KF) represents a location as a Gaussian with a mean and a covariance matrix, that can be used to express a location as a sphere but not as a spherical shell. Therefore the use of KF is not appropriate for this problem.

Several range-only localization methods have been reported in the literature (Vaganay et al., 2000; Newman and Leonard, 2003; Olson et al., 2006; Webster et al., 2009; Wang et al., 2013; Blanco et al., 2008). However, those methods are demonstrated offline after the vehicle is recovered and no online localization is performed.

In order to simplify the problem from 3D localization to 2D, we project the measured ranges *rng* (8) to the horizontal plane according to the depths of the DS $z_{DS}$ and vehicle $z_V$ (see Fig. 7). The beacon depth is known *a priori*, since it is measured during the DS deployment or by the internal pressure sensor installed in the DS, which broadcasts measures through the acoustic modem. Likewise, AUV depth information is known very precisely from its pressure sensor, only having to take into account the tide if necessary, for which appropriate models are already available (Ray, 1999).

$$\boldsymbol{z}_k^{rng} = \left[\sqrt{rng^2 - (z_V - z_{DS})^2}\right] \tag{8}$$

During the estimation of the beacon position, we rely on the on-board DR navigation filter explained in Section 3. The DR navigation drift is not taken into account because the time needed to localize the DS is small enough, as demonstrated in Vallicrosa and Ridao (2016) where a 3D sum of Gaussian (SoG) filter with active localization (AL) was used to successfully localize an acoustic beacon in a real scenario.

At known depth, a range measurement describes a beacon as being in any position on a circumference around the AUV with a radius equal to the projected range and thickness equal to the uncertainty of the measurement. To cover this big space of possibilities one might use a particle filter (PF) to represent the static beacon position, however, the PF solution would leave empty spaces without coverage. To avoid that, a much

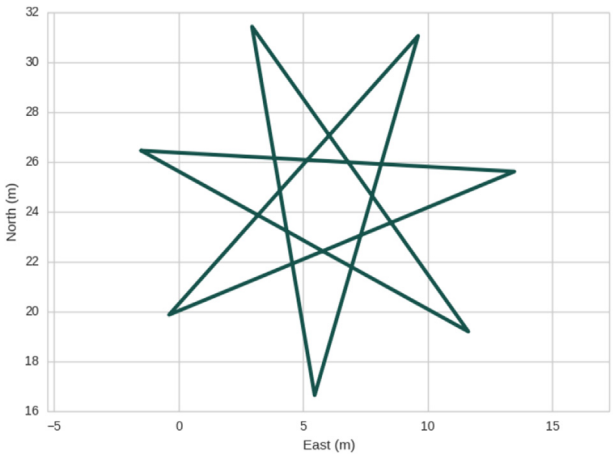


**Fig. 9.** Star shaped trajectory used for beacon localization.

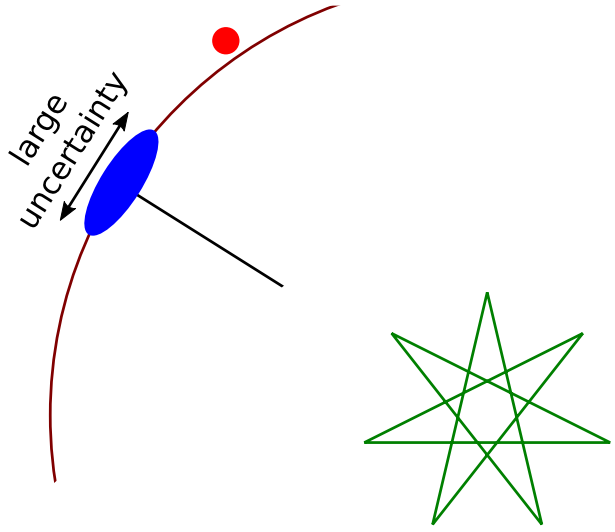


**Fig. 10.** After performing the star-shaped trajectory (green), the beacon is localized (blue) with big uncertainty on the axis tangent to the circumference described by the range measurements (dark red). An extra waypoint (red) is commanded to the vehicle to correct this uncertainty. (For interpretation of the references to color in this figure legend, the reader is referred to the Web version of this article.)

larger number of particles could be used, but then the problem would become computationally intractable. A more elaborate option is the use of a SOG filter (Blanco et al., 2008), which is similar to the PF but uses weighted Gaussians instead of weighted particles. It represents the believed beacon position $\mathscr{B}$ according to the odometry $\boldsymbol{x}_k$ and the measurements $\boldsymbol{z}_k^{rng}$:

$$p(\mathscr{B}|\boldsymbol{x}_k, \boldsymbol{z}_k^{rng}) \approx \sum_{i=1}^{N} v_k^i \mathscr{N}\left(\boldsymbol{z}_k^{rng}; \boldsymbol{\mu}_k^i, \Sigma_k^i\right), \tag{9}$$

where $v_k^i$ is the weight associated with each Gaussian, and $\boldsymbol{\mu}_k^i$ and $\Sigma_k^i$ its mean and covariance matrix.

The Gaussians in the SOG can cover all the probability space if they are correctly distributed. Moreover, an EKF is used to correct their position according to the measurements, thus improving its performance.

The SOG is initialized with the first range measurement (see Fig. 8). The filtering is carried out in two main steps. First, the range measurement is used to update each of the Gaussians ($\boldsymbol{\mu}_k^i$, $\Sigma_k^i$) with an EKF. Second, the weights are updated with the innovation of the EKF

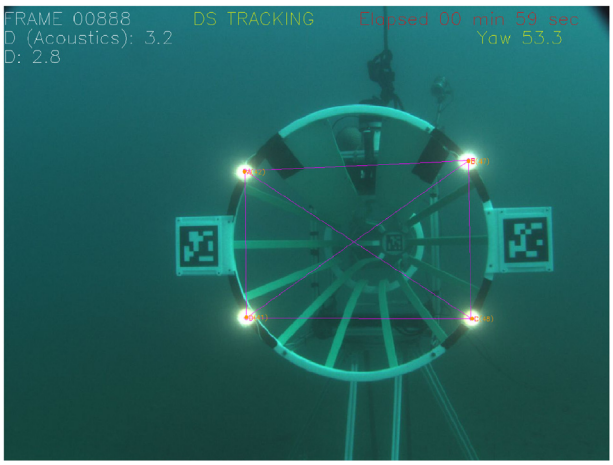


**Fig. 11.** Screenshot of the output while tracking the DS. In orange the position of the light markers according to the image analysis. In purple, the position of the markers in the DS according to the estimated relative position. AR markers were used as a complementary resource during the final approach when the light beacons are not in the FOV of the camera. (For interpretation of the references to color in this figure legend, the reader is referred to the Web version of this article.)

$\boldsymbol{y}_k^i = \boldsymbol{z}_k^{rng} - h^{rng}(\boldsymbol{\mu}_k^i)$:

$$v_k^i = v_{k-1}^i \cdot \exp\left(-\left(\boldsymbol{y}_k^i\right)^2\right), \tag{10}$$

being $i$ the index of the Gaussian and $v_{k-1}$ the previous weight. This computed weight is always in the $[0, 1]$ range. The weights of the Gaussians with a small innovation are significantly greater than those having a large innovation. Thus, after some updates, the Gaussians which are not consistent with the observed ranges become negligible while those consistently compatible will influence the estimated pose of the beacon.

When the vehicle follows an observable path (Vaganay et al., 2000), the beacon is localized in a few seconds. In this work, a simple approach using a star shaped trajectory is used to avoid symmetries and locate the beacon (see Fig. 9). The trajectory is scaled proportionally to the first measured range and it is aborted as soon as the beacon is localized with an uncertainty below a user-provided threshold.

The obtained localization of the DS after the star trajectory, suffers from a large uncertainty on the tangent of the circumference defined by the range measurements (see Fig. 10). To reduce this uncertainty before attempting to approach the DS, the vehicle is commanded to a new waypoint computed on the principal axis of the localized beacon. Range updates obtained from this position further reduce the uncertainty of localization, ending with a much better localization result.

### 3.2. Visual pose estimation

Acoustic localization can be very effective from medium to long distances, but it is not so advantageous at short distances when high precision operation is required for successfully completing the docking maneuver. To achieve a level of performance capable of ensuring the vehicle's safety during the terminal homing, visual sensing is used to provide updates with small uncertainty and high update rates.

The proposed solution consists in placing a set of active light beacons in distinct and known positions of the DS (see Fig. 11). Using a standard camera it is possible to detect the lights in the images and estimate the pose between the DS and the camera. It is worth noting that differently from range-only localization, this method is able to provide information on the relative orientation of the DS, involving the full 6 DoFs (three relative translations and three rotations).

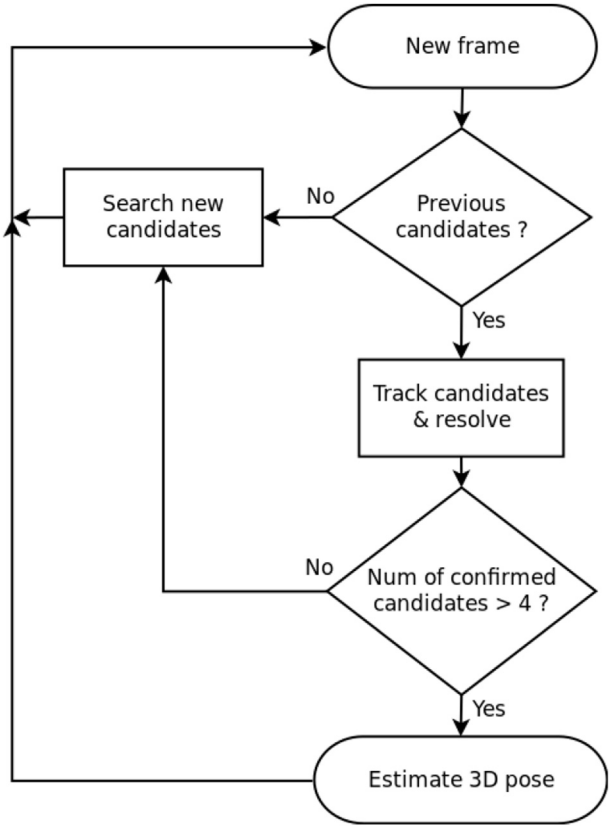


**Fig. 12.** Diagram of the detection algorithm. The algorithm starts by detecting spots in the images as candidate lights. These candidates are then tracked during several frames before deciding if they are accepted as a light beacon or rejected. Once there are four accepted candidates each one is associated to one of the light beacons and the relative pose of the DS is estimated.

With the aim of facilitating the detection of the light beacons and avoiding wrong identifications, the lights follow a known blinking pattern (as explained in Section 2). This pattern allows the actual lights to be correctly identified even in the presence of reflections or permanently illuminated areas in the scene.

The implemented detection technique is similar to the one detailed in Bosch et al. (2016), where we used it to track multiple AUVs for cooperative navigation in real sea conditions, and proved to be both effective and robust. It is based on three main steps: first there is a selection of candidate spots in the image based on gradient information. Then, at every incoming frame, the candidates are tracked taking into account the camera motion and we check its agreement along time with the known blinking pattern. Finally, each candidate is associated with a beacon according to the known geometry of the beacons installed in the docking station.

When the four lights have been detected (see Fig. 12), the relative landmark pose $\widehat{\boldsymbol{l}}$ of the DS that best fits the observation of the light beacons in the image, $\boldsymbol{q}_i$, is found using non-linear least squares minimization. This is done by searching for the values of the variable $\boldsymbol{l}$ that minimize the re-projection error of the beacons; that is, the difference between the real observation and the projection of the light beacon derived from the variable $\boldsymbol{l}$ and the calibration parameters of the camera.

$$\widehat{\boldsymbol{l}} = \arg\min_{l} \sum_{i}^{n} (f_i(\boldsymbol{p}_i) - \boldsymbol{q}_i)^2. \tag{11}$$

The variable $\boldsymbol{l}$ contains the complete pose of the DS with respect to the camera $\boldsymbol{l} = \begin{bmatrix} l_x^c & l_y^c & l_z^c & l_\phi^c & l_\theta^c & l_\psi^c \end{bmatrix}^T$. The function $f$ computes the image projection of each marker $i$ given $\boldsymbol{l}$ and the position of the marker in the DS reference frame, $\boldsymbol{p}_i$. This function uses the pinhole camera model (Zhang, 2000; Hartley and Zisserman, 2004), and assumes known intrinsic calibration parameters. Although an approximate linear solution can be found for four or more light markers using a different pose parametrization, we are interested in the above parametrization since it can be directly used in the docking problem. The problem is solved with the Levenberg-Marquardt algorithm available in the Ceres library (Agarwal et al., 2012). As with all iterative methods, it needs an initial guess of the variables, which can be approximated from the range measurements between acoustic modems. Further details on the pose estimation problem and its performance with a varying number of light beacons can be found in Gracias et al. (2015).

For the proper operation of the navigation filter it is essential to have an estimate of the pose uncertainty. A first-order approximation of the pose covariance $\Sigma_{\widehat{l}}$ can be computed from the assumed covariance $\Sigma_q$ of the pixel location of the beacons in the image and from the Jacobian $J(\widehat{\boldsymbol{l}}) = \frac{\partial g}{\partial l}(\widehat{\boldsymbol{l}})$ that relates small changes in the pose parameter with small changes in the observations. The Levenberg–Marquardt implementation provides an estimate of this Jacobian at the end of the minimization. The pose covariance estimate is given by:

$$\Sigma_{\widehat{l}} = \left( J(\widehat{\boldsymbol{l}})^T \Sigma_q^{-1} J(\widehat{\boldsymbol{l}}) \right)^{-1}. \tag{12}$$

The uncertainty obtained $\Sigma_{\widehat{l}}$ excludes the uncertainty in the transformation between the camera and the AUV and the uncertainty related with the camera calibration.

In order to have an approximate value of the uncertainty of the localization of a light in the image $\Sigma_q$ we assume the detected lit region on the image follows a 2D Gaussian distribution, and that its area covers the 95% of lit pixels. In other words, we find an equivalent radius for the blob as it was a perfect circle and we assume this radius is $2\sigma$. After analysing multiple series of light beacon images gathered at different distances and lighting conditions this value has been set as constant for the range of operation of the detector $\sigma = 1$ *pixel*.

A complementary system has been developed to help the vehicle in the last few meters of the terminal homing, when due to the small distance to the DS, the light beacons are not in the field of view of the camera. This system consists in detecting augmented reality (AR) markers placed in known positions of the DS (see Fig. 11), and estimating the relative pose of the DS in a analogous way as done with the light beacons. Notice that when the vehicle is well aligned to the docking during the terminal homing, it is capable of docking reliably using only its own navigation and the last estimated pose of the DS obtained from the light beacons localization. However, in cases where there is significant navigation drift (e.g., bad DVL readings due to slopes or rocky areas), the vehicle might not present a good alignment with the dock entry therefore causing some light beacons to drop off the field of view. In such situations, the side markers become useful to locate the DS during the last meters. It is important to note that the pose estimation based on AR markers is complementary but not a substitute to the light beacon approach given that it only works when there is ambient or artificial light to make the markers visible and that the distance under which the AR markers are detectable is significantly smaller (see Section 5, Results). The detection of the AR markers was done using the ARUCO library (Garrido-Jurado et al., 2014). Given that the library does not provide any uncertainty values on the location of the detected marker corners, a conservative value of $\sigma = 2$ *pixel* was chosen. This uncertainty was then propagated in the same way as in the case of the light beacons to obtain $\Sigma_{\widehat{l}}$.

## 4. Vehicle operation and control

The goal of the LOON-DOCK project is to have a vehicle persistently deployed so that a user can connect to it and use it remotely to carry out

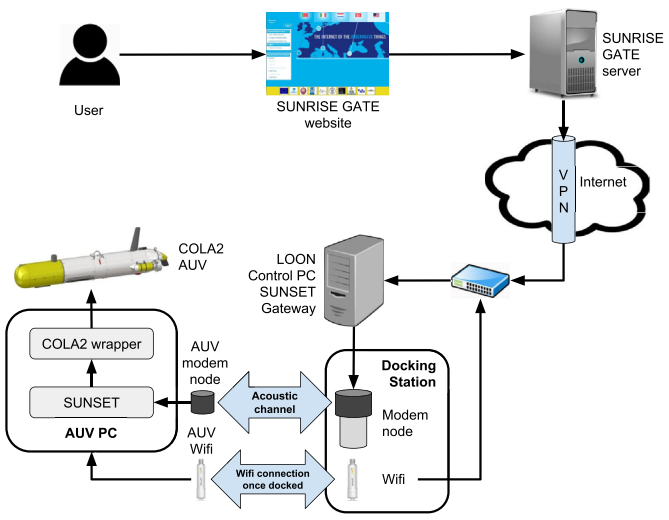


**Fig. 13.** Diagram of the connections to remotely operate the DS/AUV system in the LOON testbed.

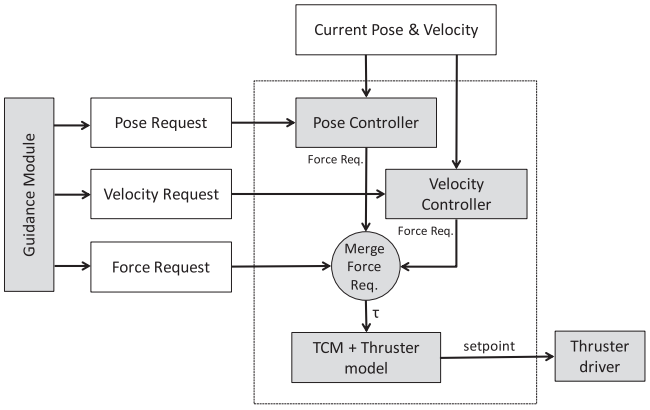


**Fig. 14.** Girona 500 AUV control scheme.

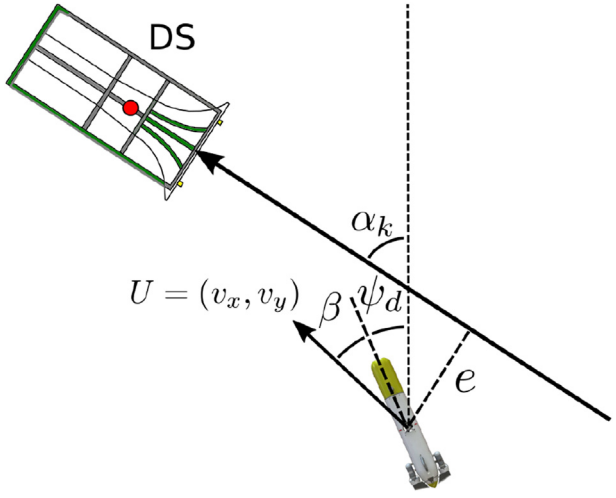


**Fig. 15.** Angles and distances involved in the LOS controller.

survey-like missions. Therefore, the user must be able to define, upload and delete mission plans to the AUV and start, stop or abort its execution. These plans have been defined to include the following motion commands: go to a position, keep the current position, execute a lawnmower like trajectory, and dock or undock. Moreover, the user can request the AUV position and state as well as information related with the AUV payload in real time. Acoustic modems are used to carry out all these communications, however, when the AUV is docked, the user can download the data gathered in a previous mission using the WiFi connection installed in the DS.

The following sections present the communication framework used to remotely operate the AUV and the high-level and low-level controllers used to carry out the mission plans defined by the users.

### 4.1. Remote operation

As shown in Fig. 13, a user can connect to the control PC in the LOON test-bed using the web-based interface named SUNRISE GATE (Petrioli et al., 2014), passing through a virtual private network (VPN) and a gateway that ensure the privacy and security of the network (Alves et al., 2014). The commands that the user executes through the web interface are received by the control PC and translated to SUNSET commands (Petrioli et al., 2015), which is the protocol used for acoustic communications. Then, they are sent through an acoustic node (i.e., the modem mounted in the DS and wired to the control PC) to another acoustic node (i.e., the modem of the AUV). Because the AUV uses a ROS-based architecture, (Quigley et al., 2009), once it receives these commands, they are translated from SUNSET to ROS. Finally, a *wrapper* module executes the necessary vehicle primitives available in the Sparus II control architecture named component oriented layer-based architecture for autonomy (COLA2) (Palomeras et al., 2012).

Both the SUNRISE GATE and the SUNSET communications were previously developed in the context of the SUNRISE project. Therefore, the main effort to allow the execution of remote commands to Sparus II AUV has been to map the SUNSET commands to the primitives in the COLA2 architecture used in the vehicle.

### 4.2. AUV guidance and control

To execute the plans defined by a user, the COLA2 architecture implements a high-level guidance module with the following motion commands: *keep position*, *go to waypoint*, perform a *survey-like pattern* and *dock/undock*. To achieve these motion commands the control architecture has a low-level module including a velocity (linear and angular) and a pose (position and orientation) tracking control schemes (see Fig. 14).

The objective for the velocity control scheme is to minimize the error between a commanded velocity setpoint and the actual vehicle velocity. Analogously, the pose tracking controller seeks to minimize the error between a desired pose setpoint and the actual vehicle pose. Both pose and velocity controllers generate an output force ($\tau_i$) that is merged with other forces that can be generated by other high-level controllers (e.g., safety controllers, teleoperation, etc.). The resulting force ($\tau_d$) must be then achieved by the vehicle thrusters. To compute the thrust that each propeller must yield, $\tau_d$ is multiplied by the inverse of the thruster control matrix (TCM), being TCM a matrix that codifies the amount of force that each thruster produces per DoF. A complete description of the implemented low-level controller module can be found in Palomeras et al. (2015) for an AUV that runs the same architecture than Sparus II AUV.

To implement the available motion commands, the guidance module uses the pose and velocity control schemes as follows:

*Station Keeping:* To keep the current position, the pose of the AUV in the moment to enable this motion command is sent as a desired setpoint to the pose controller.

*Go to waypoint:* To move the AUV to a specific waypoint, the guidance module computes the orientation error ($\psi_e$) between the vehicle's current position and the desired waypoint and sends the desired yaw ($\psi_d$) to the pose controller together with the desired depth ($z_d$). When, $\psi_e$ is smaller than a defined error, the desired surge ($u_d$) is computed, proportionally to $\psi_e$ and a maximum speed, and is sent to the velocity controller.

*Survey like pattern:* A lawn-mower pattern is generated from the user

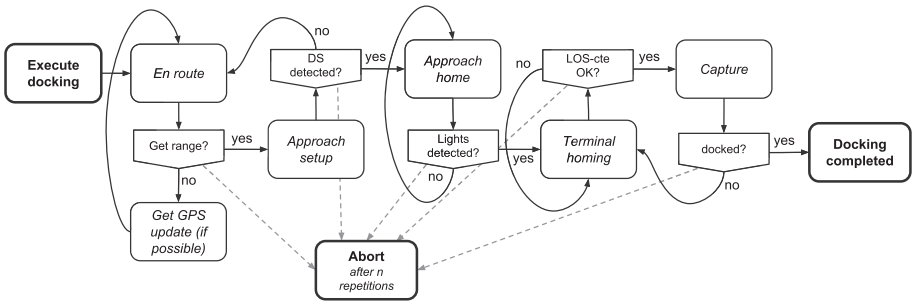


**Fig. 16.** State diagram for undocking, mission execution, and docking while handling more common failures.

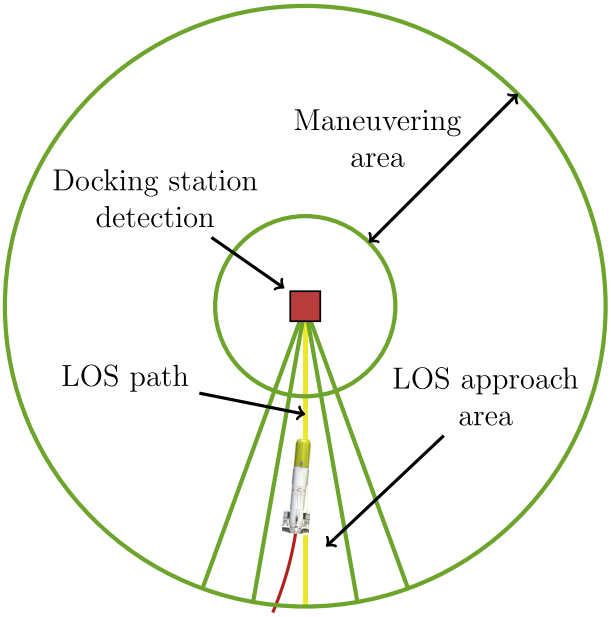


**Fig. 17.** Terminal homing phase.

input specifying the area to be covered (i.e., three waypoints) and the desired track spacing. The generated transects are then followed using a line-of-sight (LOS) controller with cross tracking error (LOS-cte), as the one described in Fossen (2011). A proportional controller using the cross-track error $e$ in conjunction with the sideslip (drift) angle $\beta$ (13) allows steady state convergence of the controller under constant currents (see Fig. 15). The LOS-cte controller sends the computed yaw reference $\psi_d$ and the desired depth $z_d$ to the pose controller while the desired constant surge velocity $u_d$ is achieved by the velocity control scheme.

$$\psi_d = \alpha_k + arctan\left(-K_p\, e\right) - \beta \tag{13}$$

$$\beta = arctan2(v_y, v_x)$$

*Docking:* Finally, for the docking motion command, the guidance module executes a state machine like the one presented in Fig. 16:

i Given an estimation of the DS position and orientation, a waypoint 40 m in front of it is computed and the AUV navigates to it (*en route*). Notice that this point is only used to start sensing ranges from the modem and therefore the accurate positioning of the AUV in that point is not critical. It is set at 40 m in order to account for up to 30 m of navigation drift. In this way there is enough margin to avoid potential collisions with the DS while still ensuring that ranges would be sensed with no problem (even at shallow water, i.e., less than 15 m depth, ranges can be heard at more than 70 m distance). In the event that no ranges were detected by the modem from this point, the AUV surfaces to get a GPS update, if possible, and moves again to the computed location.

ii Once ranges are available, the acoustic localization algorithm (see Section 3.1) is enabled in order to estimate the DS position (*approach setup*).

iii Once the acoustic localization finalizes, if a candidate position for the DS is obtained, the AUV is sent several meters in front of it and a visual-based searching procedure, consisting in turning the vehicle left and right while approaching the DS up to a safety distance, is started to localize the light beacons (*approach home*).

iv If the light beacons are localized (see Section 3.2), the DS landmark is initialized in the EKF-SLAM filter and the vehicle is sent again to some distance with respect to the DS entrance to carry out the *terminal homing*. This phase can be classified as a pose-based visual servoing (PBVS) and contains two main steps (see Fig. 17): move closer to the LOS path while not losing the visual contact with the DS and follow the LOS path until reaching the DS entrance. Initially, if the vehicle is not aligned with the DS, a series of movements might be required to position the robot in an appropriate location. These maneuvers always try to keep the light beacons inside the camera FOV using the position of both the AUV and the DS estimated by the navigation filter. In the second step, the already presented LOS algorithm with cross tracking error (LOS-cte) is executed to guide the AUV up to the DS entrance. If the AUV gets out of the LOS approach area while getting closer to the DS it returns to the first step.

v If the *terminal homing* finalizes successfully, the *capture* phase starts applying a force profile to the thrusters to gently introduce the vehicle inside the DS. A similar force profile, but on the opposite direction, is applied to undock the vehicle.

If all phases conclude satisfactory, to verify that the vehicle has been correctly docked, several elements are considered: a camera in the DS pointing to the funnel, the WiFi connection between the DS and the AUV, and also a test to check that the AUV orientation is static despite applying some thrust.

If any of the phases fails, the same phase or the previous one is repeated as shown in Fig. 16. If after three repetitions the phase keeps failing, the docking command is aborted.

## 5. Experiments and results

All the elements described in Section 3 were tested incrementally. Preliminary tests were performed in a $16 \times 8$x5m water tank at the University of Girona. Even though this water tank has a rather limited space, it provides a convenient and controlled environment with a supervision room that offers direct view to the water. In there we could test the light beacons localization, the acoustic communications using SUNSET, the vehicle remote operation from the SUNRISE GATE, and the final phases of the docking maneuver (i.e., *approach home*, *terminal homing* and *capture*). Later, additional experiments were carried out in a harbour near Girona. The SOG filter and further tests on the light beacon localization system were performed at this harbour under more real conditions. Once

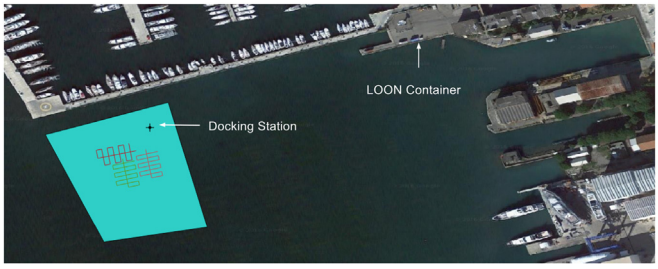


**Fig. 18.** View of the operational area, where the docking station was deployed and the experiments took place. All tests were controlled from a lab container located next to the LOON container.

all the phases of the docking command were checked individually, more complete tests, involving survey trajectories started and/or ended in the dock, were carried out using the acoustic communications between the DS and the AUV.

Final experiments were performed at the LOON testbed, located in La Spezia (Italy), during a three day campaign. Fig. 18 shows the location of the LOON container, where the LOON control PC running the SUNSET gateway was located. The blue area shows the region that was designated for conducting the experiments and where the DS was installed at around 9 m depth. Fifteen mission plans, all of them including docking commands, were executed by the AUV at this testbed.

In all tests the DS was correctly detected and only in three (20%) was not possible to conclude the docking maneuver due to the presence of strong water currents that affected the DS area during some hours in a direction that was not aligned with the docking station. In two of these three cases, after a predefined number of re-attempts, the system returned an error indicating that the docking could not be performed and in the remaining one, the vehicle finalized the maneuver but detected that the vehicle was not correctly docked. As described in Section 2, the DS can rotate to be aligned with the water currents. However, in the DS current state, this is a manual adjustment that has to be done by a diver. When the current was aligned with the DS axis or was relatively low (below 0.15 m/s), the docking maneuver was always successful despite very poor visibility (below 3 m most of the time).

Several tests were done to assess the remote operation of the vehicle. First, SUNSET commands were sent through the SUNSET user interface directly from the LOON control PC. Once checked that the AUV could be completely commanded by sending acoustic orders through the SUNSET protocol, the vehicle was remotely operated through the SUNRISE GATE web interface demonstrating the complete integration with the LOON test-bed (see Fig. 19). The DS capability to latch the AUV and to transmit large amounts of data once this was docked was also tested during the trials allowing to keep the AUV docked, in suspension mode, for several hours as well as to transmit previously gathered data files up to 45Mbits/s.

Fig. 20 summarizes one of the full missions performed by the AUV. The vehicle started by undocking from the DS (purple line) and went to the first waypoint of the survey trajectory. It executed the grid survey (orange line) while gathering multibeam data from 5 m altitude. At the end of it, the docking motion command was triggered. Even though the AUV had left the DS, and therefore it could receive acoustic range updates during the whole mission, we forced the AUV to localize the DS using the SOG filter with AL. Thus, the AUV started the star pattern trajectory that is performed to increase the observability of the DS ranges.

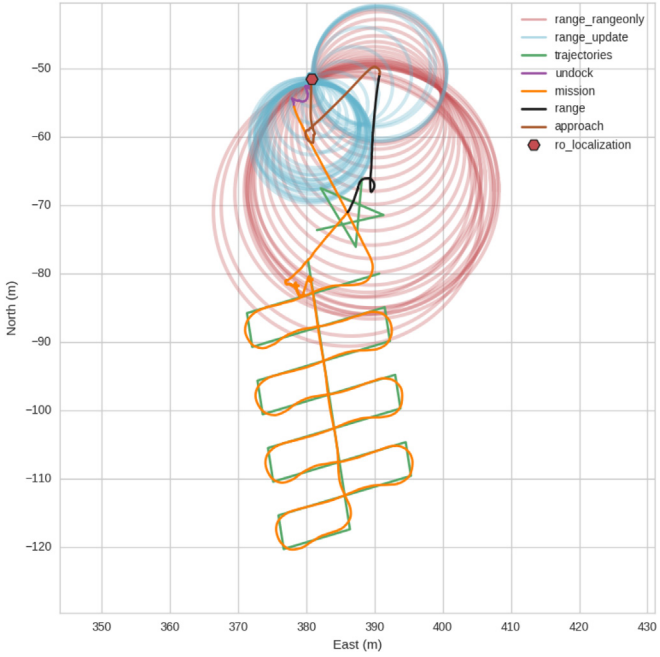


**Fig. 20.** Visual mission summary.

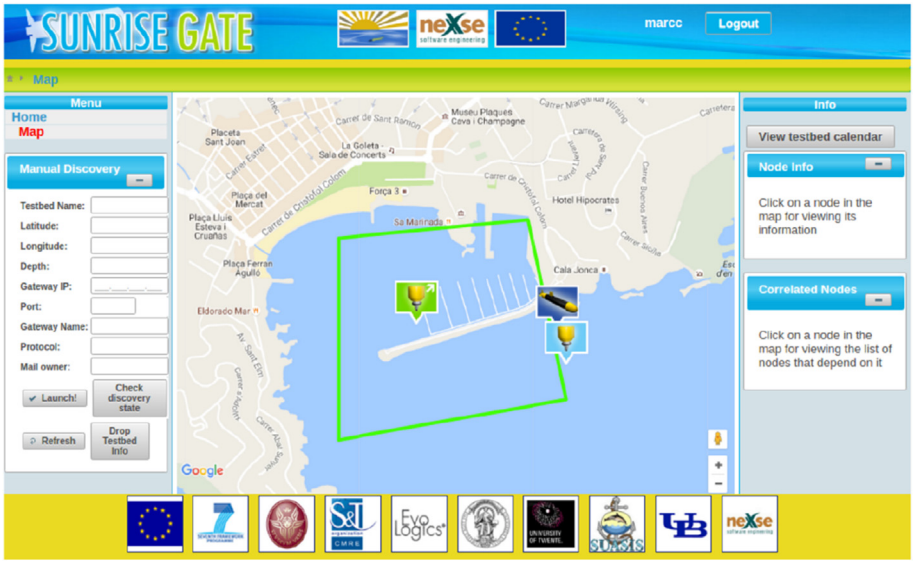


**Fig. 19.** SUNRISE GATE web interface screenshot.

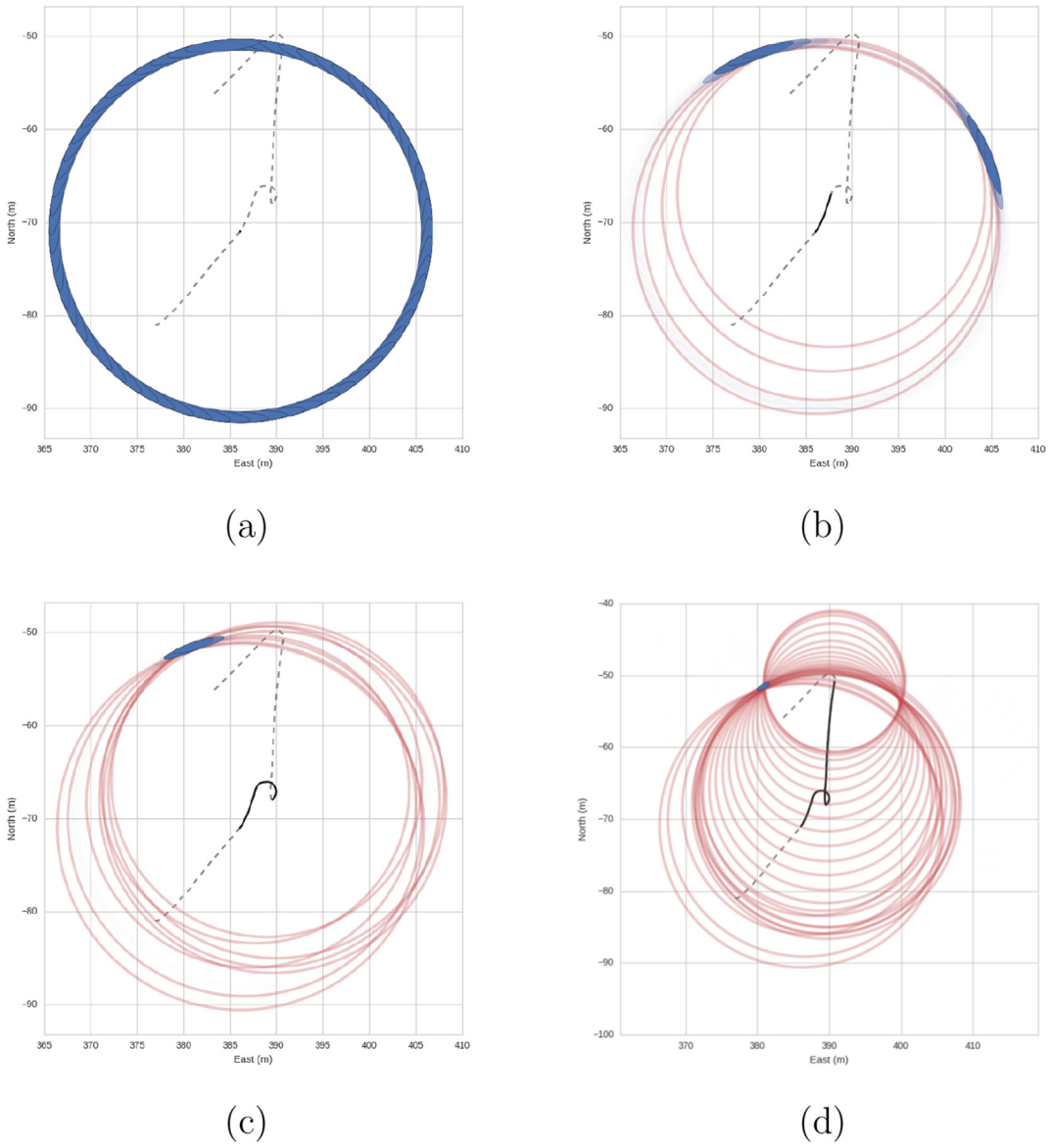


**Fig. 21.** Evolution of the range-only localization algorithm to detect the docking station position. See text for details.

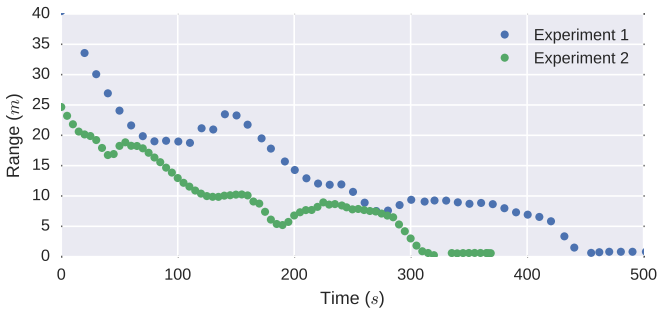


**Fig. 22.** Range measurements over time for two different missions.

The range-only localization process can be seen in more detail in Fig. 21. The algorithm starts by initializing a set of Gaussians that cover all the position probability space (Fig. 21a) according to the first range measurement. The vehicle initiates the star pattern trajectory and the incoming range measurements quickly narrow the probability of the DS position to two possible locations that are in agreement with all the received measurements (Fig. 21b). After performing the first turn, new incoming ranges narrow down the uncertainty of the docking station position below the established threshold ($\sigma_{th} = 1.5$). At this point, the vehicle moves to one side of the determined position in order to decrease the uncertainty of the ellipse (down to $\sigma_{DS} = 0.7$) in its main axis (Fig. 21c and d). It is worth noting that this successful localization benefited from very consistent range measurements provided through SUNSET, arriving every 5s.

Range measurements can be affected by various types of non-Gaussian noise like surface bounces, wrap returns and background noise (Yoerger et al., 2007). In the presented experiments, the measured ranges are not affected by those problems due to the small distance between the AUV and the DS and because there were no obstacles in the vicinity, leaving a direct reception for modem communication and range measurements. This correct reception can be observed in Fig. 22 where measured ranges over time, during the localization and approach to the DS, show a smooth shape without outliers. Given the favorable conditions, the range update rate was constant at 0.2 *Hz*.

In the final approach to the docking station, the optical tracking system is started in order to have a better precision on the DS location as well as a faster update rate. At this point, the docking command executes

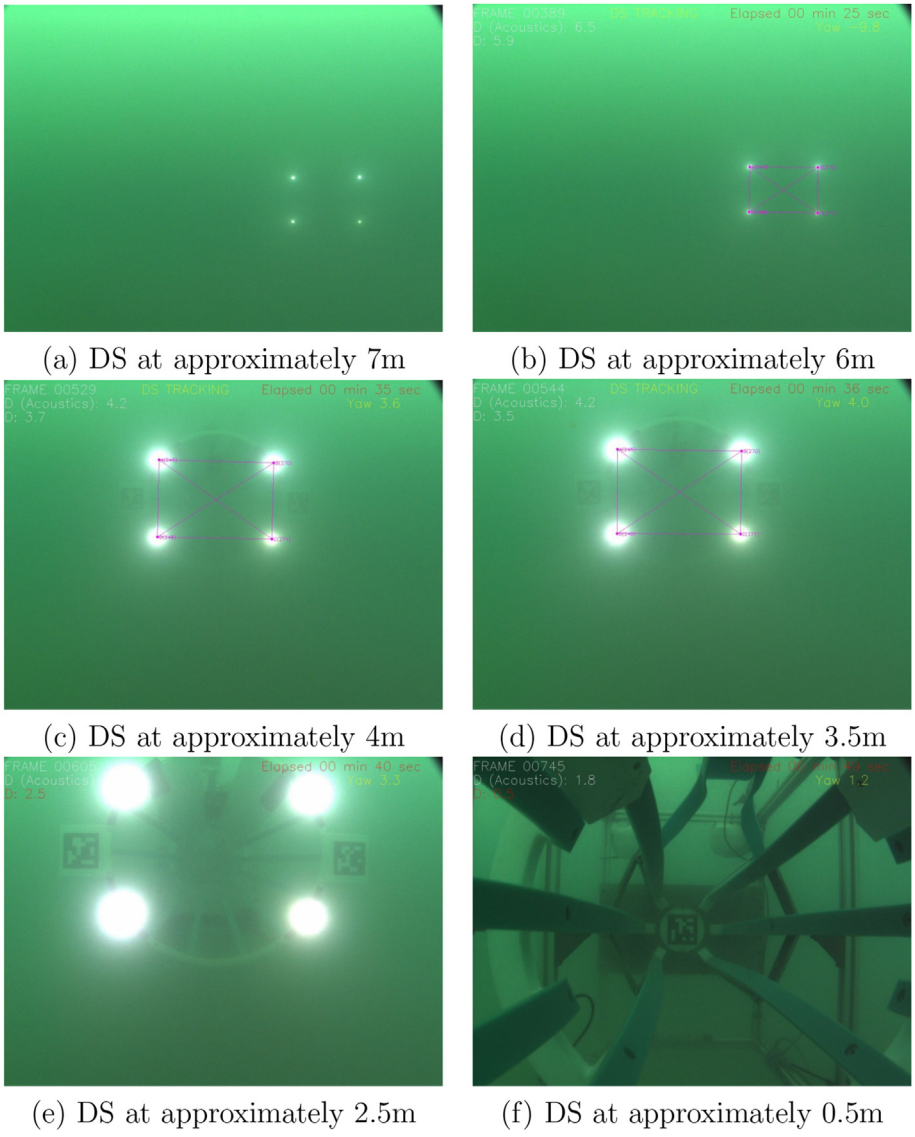


**Fig. 23.** Docking maneuver images from Sparus II AUV on-board camera. The lights were visible from at least 7 m away from the DS, while the AR markers were only visible at 3 m.

a search pattern in which the AUV approaches the estimated position of the DS from 10 m to 4 m, and every 2 m the AUV performs a sweeping movement turning from 90deg to the left to 90deg to the right. This behavior terminates when the DS is detected. With this simple search pattern, we ensure that the vision-based system will be able to detect the light beacons, even when the error in the SOG filter estimation is up to 2.8 m (i.e., 95% of cases when $\sigma = 0.7$).

The maximum distance of operation for the optical tracking depends strongly on the visibility conditions. For this particular experiment, the visibility was considered poor: the structural elements of the DS were not visible at distances greater than 3 m. However, the light beacons could be properly detected up to a maximum distance of 7 m, allowing to complete the docking approach without difficulty. Visibility conditions can be appreciated in Fig. 23.

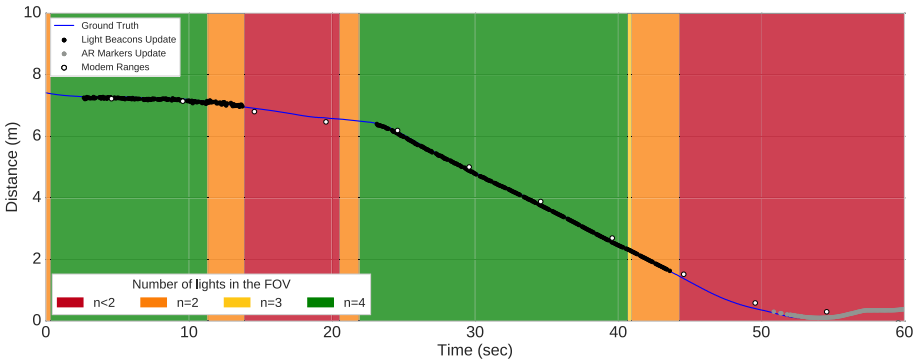


**Fig. 24.** DS tracking performance during the docking command execution in one of the missions. The different colored dots represent three different updates: White dots correspond to acoustic updates, black dots are visual updates computed using light beacons while grey dots are visual updates computed using AR markers. The blue line represents the relative distance between the DS and the AUV according to the navigation of the vehicle and was computed offline once the position of the DS was known precisely. The colored background reflects how many light beacons were inside the FOV of the camera according to the orientation of the vehicle. (For interpretation of the references to color in this figure legend, the reader is referred to the Web version of this article.)

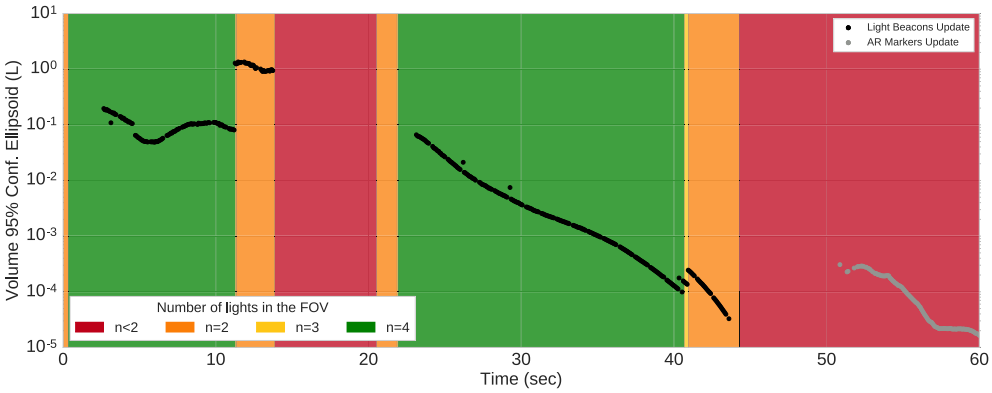


**Fig. 25.** Uncertainty of the optical tracking updates during the docking maneuver in one of the missions. Black dots correspond to light beacons updates while grey dots are for AR markers updates. The colored background reflects how many light beacons were inside the camera FOV according to the vehicle's orientation.

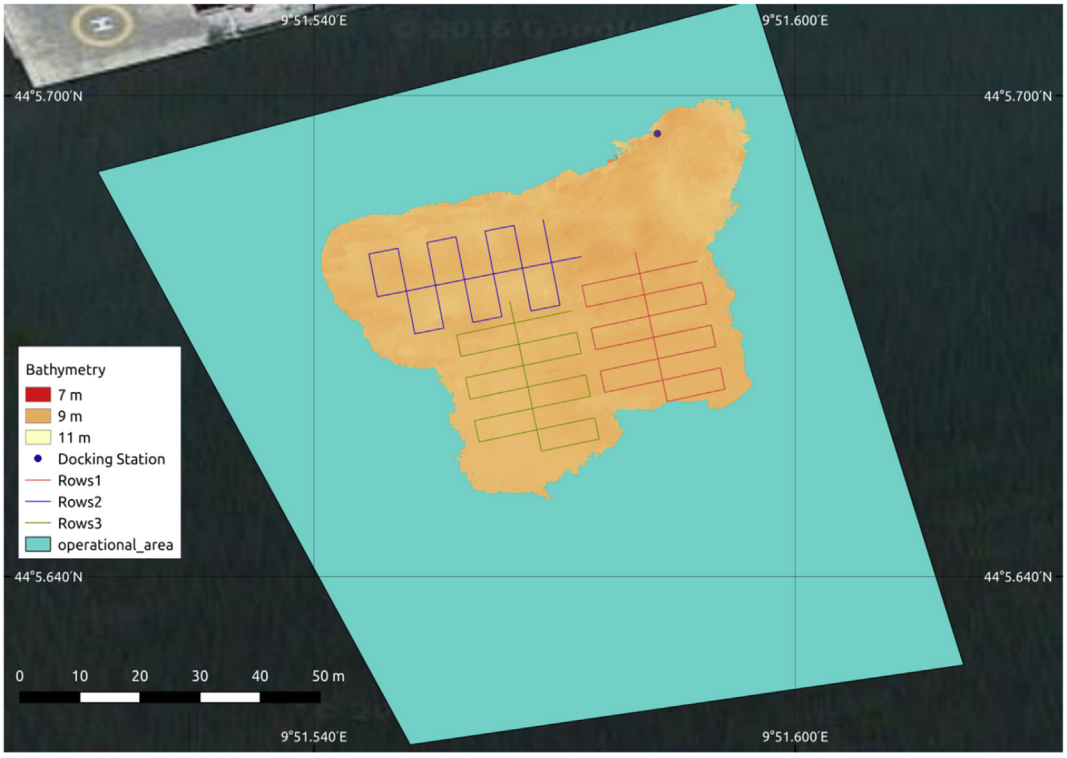


**Fig. 26.** Bathymetric data collected during different experiments in the LOON testbed.

Once the vision-based system is able to estimate consistently several times the DS pose, a landmark is initialized in the EKF localization system and every time that a new vision-based measure or a range measure is obtained, the position of both AUV and DS is updated in the navigation filter (see Section 3). After introducing the landmark in the EKF, the guidance module moves the AUV to a waypoint placed 10 m in front of the DS pose available in the state vector and initializes the terminal homing phase. While approaching the DS following the LOS path, if the estimated distance by the optical tracking is under 1.5 m and there is ambient light, the approach used to detect the DS changes and the algorithm tries to estimate the relative position of it using the AR markers instead of the light beacons. When the system was on tracking mode, it was able to provide updates at a maximum of 15 *Hz*, which corresponds to the capture frame rate of the camera. Because acoustic ranges, light beacons, and AR marker measurements are equally used to update the DS position in the EKF-SLAM filter, the position of these three elements with respect to the DS frame must be properly calibrated.

Fig. 24 compares the distance between the AUV and the DS estimated according to the acoustic ranges, light beacons and AR markers. All methods show a high degree of agreement with the trajectory estimated offline, once the DS position was known precisely, with differences smaller than 30 cm. The background colors in the plot represent the number of light beacons inside the FOV of the camera, this is, depending on the orientation of the AUV a different number of light beacons are inside the FOV of the camera. Due to the fact that the orientation of the DS is known *a priori*, even when only two of the light beacons have been identified it is possible to estimate the relative pose. For this particular mission the optical track was lost between seconds 15 to 25 due to a reorientation of the AUV to correctly approach the DS. From second 45 onwards, when the distance is smaller than 1.5 m, the optical tracking was based on AR markers.

From the plot, we can conclude that the optical tracking worked when the lights were in the camera FOV and in a distance of less than 7 m. The tracking was lost at 1.5 m, moment in which the tracking method changed to AR markers detection.

The uncertainty of the DS position according to the visual estimates is shown in Fig. 25. The plot includes the uncertainty in the detection of the DS in the image, but excludes the uncertainty in the transformation

between the camera and the AUV and the uncertainty related with the camera calibration. Peaks in the uncertainty plot appear when only two or three lights are visible instead of four.

Fig. 26 shows the bathymetric data collected along several survey missions that were autonomously commanded and executed in different locations. Although the data might not be very valuable in terms of mapping utility, because the area was extremely flat and with scarcity of features, it serves as a proof of concept and testifies to the whole concept of the LOON-DOCK: being able to remotely command and retrieve large amounts of data from a persistently deployed AUV through a DS.

## 6. Conclusions and future work

This paper has presented the docking solution implemented in the context of the LOON-DOCK project in order to demonstrate the remote operation and data transmission of a survey-AUV from Internet.

We have designed and built a docking station for Sparus II AUV, providing passive and active guidance mechanisms, a latching system, high-bandwidth data communications and visual feedback. The active guidance for docking is based on two complementary and cost-effective systems: two acoustic modems using only range information within a SOG filter to detect the DS from mid distances and a vision-based system, composed of a set of light beacons and visual markers, used in the terminal homing phase. The combination of a mid-accuracy mid-range method with a high-accuracy short-range method allows us to reliably dock the AUV.

The system has been extensively tested, with trials ranging from a controlled water tank environment to more realistic sea operation conditions. Successful validation of all the involved parts (i.e., AUV navigation, control, acoustic communications, and autonomous docking capabilities) has been conducted despite the presence of currents and very poor water visibility.

The main downside identified in our docking approach arises in the presence of strong water currents that are not aligned with the docking station. Sparus II, being a torpedo-shaped vehicle underactuated in sway, can only deal with lateral currents by changing its heading. This has two negative effects: first, by adapting the heading to compensate the currents, the vehicle is more prone to lose sight of the light beacons during the terminal homing, and second, if the misalignment with the docking is larger than 30°, the vehicle cannot physically enter inside the funnel receptacle. For this reason, as a future work, it is important to deal with the automatic alignment of the DS with the currents. Notice that the proposed design is already able to rotate the DS funnel receptacle and only a system to measure the water currents and an actuator to move it accordingly would have to be added. Besides, a battery recharging mechanism will be also integrated in the future to complete the system and enable its persistent deployment through longer time spans.

## Acknowledgement

This work was supported by the EU funded project LOON-DOCK/SUNRISE (Sensing, monitoring and actuating in the UNderwater world through a federated Research InfraStructure Extending the Future Internet) FP7-ICT-2013-10-611449.

## References

Agarwal, Sameer, Mierle, Keir, et al., 2012. Ceres solver. http://ceres-solver.org.

Allen, Ben, Austin, Tom, Forrester, Ned, Goldsborough, Rob, Kukulya, Amy, Packard, Greg, Purcell, Mike, Stokey, Roger, 2006. Autonomous docking demonstrations with enhanced remus technology. In: OCEANS 2006. IEEE, pp. 1–6.

Alves, J., Potter, J., Guerrini, P., Zappa, G., LePage, K., Sept 2014. The loon in 2014: test bed description. In: 2014 Underwater Communications and Networking (UComms), pp. 1–4. https://doi.org/10.1109/UComms.2014.7017141.

Bellingham, James G., 2016. Autonomous underwater vehicle docking. In: Springer Handbook of Ocean Engineering. Springer, pp. 387–406.

Blanco, J.-L., Fernandez-Madrigal, J.-A., González, Javier, 2008. Efficient probabilistic range-only slam. In: Intelligent Robots and Systems, 2008. IROS 2008. IEEE/RSJ International Conference on. IEEE, pp. 1017–1022.

Bosch, Josep, Gracias, Nuno, Ridao, Pere, Istenič, Klemen, Ribas, David, 2016. Close-range tracking of underwater vehicles using light beacons. Sensors. ISSN: 1424-8220 16 (4), 429. http://www.mdpi.com/1424-8220/16/4/429.

Brignone, L., Perrier, M., Viala, C., 2007. A fully autonomous docking strategy for intervention auvs. In: OCEANS 2007-Europe. IEEE, pp. 1–6.

Carreras, Marc, Candela, C., Ribas, D., 2013. Sparus II, design of a lightweight hovering AUV. In: 5th International Workshop on Marine Technology (MARTECH), ISBN 2011728827, pp. 163–164.

Cowen, Steve, Briest, Susan, Dombrowski, James, 1997. Underwater docking of autonomous undersea vehicles using optical terminal guidance. In: OCEANS'97. MTS/IEEE Conference Proceedings, vol. 2. IEEE, pp. 1143–1147.

Curtin, Thomas B., Bellingham, James G., Catipovic, Josko, Webb, Doug, 1993. Autonomous oceanographic sampling networks. Oceanography 6 (3), 86–94.

Feezor, Michael D., Sorrell, F. Yates, Blankinship, Paul R., 2001. An interface system for autonomous undersea vehicles. IEEE J. Ocean. Eng. 26 (4), 522–525.

Fossen, Thor I., 2011. Handbook of Marine Craft Hydrodynamics and Motion Control. John Wiley and Sons.

Garrido-Jurado, S., Mu noz Salinas, R., Madrid-Cuevas, F.J., Marín-Jiménez, M.J., 2014. Automatic generation and detection of highly reliable fiducial markers under occlusion. Pattern Recogn. ISSN: 0031-3203 47 (6), 2280–2292. https://doi.org/10.1016/j.patcog.2014.01.005. http://www.sciencedirect.com/science/article/pii/S0031320314000235.

Gracias, Nuno, Bosch, Josep, Karim, Mohammad Ehsanul, 2015. Pose estimation for underwater vehicles using light beacons. In: Proc. Of the 4th IFAC Workshop on Navigation, Guidance and Control of Underwater Vehicles NGCUV 2015, vol. 48, pp. 70–75.

Hartley, R.I., Zisserman, A., 2004. Multiple View Geometry in Computer Vision, second ed. Cambridge University Press, ISBN 0521540518.

Hong, Young-Hwa, Kim, Jung-Yup, Oh, Jun-ho, Lee, Pan-Mook, Jeon, Bong-Hwan, Oh, Kyu-Hyun, et al., 2003. Development of the homing and docking algorithm for auv. In: The Thirteenth International Offshore and Polar Engineering Conference. International Society of Offshore and Polar Engineers.

Jacobson, John, Cohen, Pierce, Nasr, Amin, Schroeder, Art J., Kusinski, Greg, 2013. Deepstar 11304: laying the groundwork for auv standards for deepwater fields. Mar. Technol. Soc. J. 47 (3), 13–18.

King, Peter, Lewis, Ron, Mouland, Darrell, Walker, Dan, 2009. Catchy an auv ice dock. In: OCEANS 2009, MTS/IEEE Biloxi-Marine Technology for Our Future: Global and Local Challenges. IEEE, pp. 1–6.

Krupinski, Szymon, Maurelli, Francesco, Grenon, Gabriel, Petillot, Yvan, 2008. Investigation of autonomous docking strategies for robotic operation on intervention panels. In: OCEANS 2008. IEEE, pp. 1–10.

Kushnerik, A.A., Vorontsov, A.V., Ph Scherbatyuk, A., 2009. Small auv docking algorithms near dock unit based on visual data. In: OCEANS 2009, MTS/IEEE Biloxi-Marine Technology for Our Future: Global and Local Challenges. IEEE, pp. 1–6.

Li, Dejun, Chen, Yan hu, Shi, Jian guang, Yang, Can jun, 2015. Autonomous underwater vehicle docking system for cabled ocean observatory network. Ocean Eng. ISSN: 0029-8018 109 (Suppl. C), 127–134. https://doi.org/10.1016/j.oceaneng.2015.08.029. http://www.sciencedirect.com/science/article/pii/S0029801815004278.

Li, Dejun, Zhang, Tao, Yang, Canjun, 2016. Terminal underwater docking of an autonomous underwater vehicle using one camera and one light. Mar. Technol. Soc. J. 50, 58–68, 11.

Maire, Frederic D., Prasser, David, Dunbabin, Matthew, Dawson, Megan, 2009. A vision based target detection system for docking of an autonomous underwater vehicle. In: Proceedings of the 2009 Australasion Conference on Robotics and Automation. Australian Robotics and Automation Association.

Manley, Justin, Willcox, Scott, 2010. The wave glider: a persistent platform for ocean science. In: OCEANS 2010 IEEE-Sydney. IEEE, pp. 1–5.

McEwen, Robert S., Hobson, Brett W., McBride, Lance, Bellingham, James G., 2008. Docking control system for a 54-cm-diameter (21-in) auv. IEEE J. Ocean. Eng. 33 (4), 550–562.

Meyer, D., 2016. Glider technology for ocean observations: a review. Ocean Sci. Discuss. 2016, 1–26. https://doi.org/10.5194/os-2016-40. http://www.ocean-sci-discuss.net/os-2016-40/.

Murarka, Aniket, Kuhlmann, Gregory, Gulati, Shilpa, Flesher, Chris, Sridharan, Mohan, Stone, William C., 2009. Vision-based frozen surface egress: a docking algorithm for the endurance AUV. In: Proceedings of the Unmanned Untethered Submersible Technology Conference (UUST), vol. 2009.

Newman, Paul, Leonard, John, 2003. Pure range-only sub-sea SLAM. In: Robotics and Automation, 2003. Proceedings. ICRA'03. IEEE International Conference on, vol. 2. IEEE, pp. 1921–1926.

Olson, Edwin, Leonard, John J., Teller, Seth, 2006. Robust range-only beacon localization. Oceanic Eng. IEEE J. 31 (4), 949–958.

Palomeras, N., El-Fakdi, A., Carreras, M., Ridao, P., Oct 2012. Cola2: a control architecture for auvs. IEEE J. Ocean. Eng. ISSN: 0364-9059 37 (4), 695–716. https://doi.org/10.1109/JOE.2012.2205638.

Palomeras, Narcís, Carrera, Arnau, Hurtós, Natàlia, Karras, George C., Bechlioulis, Charalampos P., Cashmore, Michael, Magazzeni, Daniele, Long, Derek, Fox, Maria, Kyriakopoulos, Kostas J., et al., 2015. Toward persistent autonomous intervention in a subsea panel. Aut. Robots 1–28.

Park, Jin-Yeong, Jun, Bong huan, Lee, Pan mook, Oh, Junho, 2009. Experiments on vision guided docking of an autonomous underwater vehicle using one camera. Ocean Eng. ISSN: 0029-8018 36 (1), 48–61. https://doi.org/10.1016/j.oceaneng.2008.10.001. http://www.sciencedirect.com/science/article/pii/S0029801808002242. Autonomous Underwater Vehicles.

Petrioli, C., Potter, J., Petroccia, R., November, 17 2013. Sunrise "sensing, monitoring and actuating on the underwater world through a federated research infrastructure extending the future internet. In: Proceedings of EMSO 2013. Rome, Italy.

Petrioli, C., Petroccia, R., Spaccini, D., Vitaletti, A., Arzilli, T., Lamanna, D., Galizial, A., Renzi, E., Sept 2014. The sunrise gate: accessing the sunrise federation of facilities to test solutions for the internet of underwater things. In: 2014 Underwater Communications and Networking (UComms), pp. 1–4. https://doi.org/10.1109/UComms.2014.7017144.

Petrioli, Chiara, Petroccia, Roberto, Potter, John R., Spaccini, Daniele, 2015. The sunset framework for simulation, emulation and at-sea testing of underwater wireless sensor networks. Ad Hoc Netw. 34, 224–238.

Quigley, Morgan, Conley, Ken, Gerkey, Brian P., Faust, Josh, Foote, Tully, Leibs, Jeremy, Wheeler, Rob, Ng, Andrew Y., 2009. Ros: an open-source robot operating system. In: ICRA Workshop on Open Source Software.

Ray, Richard D., 1999. A Global Ocean Tide Model from Topex/poseidon Altimetry: Got99.2. Technical Report. NASA Technical Reports Server (NTRS).

Singh, Hanumant, Bellingham, James G., Hover, Franz, Lemer, S., Moran, Bradley A., Von der Heydt, Keith, Yoerger, Dana, 2001. Docking for an autonomous ocean sampling network. IEEE J. Ocean. Eng. 26 (4), 498–514.

Smith, S.M., Kronen, D., 1997. Experimental results of an inexpensive short baseline acoustic positioning system for auv navigation. In: OCEANS'97. MTS/IEEE Conference Proceedings, vol. 1. IEEE, pp. 714–720.

Stokey, Roger, Allen, Ben, Austin, Tom, Goldsborough, Rob, Forrester, Ned, Purcell, Mike, Alt, Chris Von, 2001. Enabling technologies for remus docking: an integral component of an autonomous ocean-sampling network. IEEE J. Ocean. Eng. 26 (4), 487–497.

Stone, W., Hogan, B., Flesher, C., Gulati, S., Richmond, K., Murarka, A., Kuhlman, G., Sridharan, M., Siegel, V., Price, R.M., et al., 2010. Design and deployment of a four-degrees-of-freedom hovering autonomous underwater vehicle for sub-ice exploration and mapping. Proc. Inst. Mech. Eng. Part M J. Eng. Marit. Environ. 224 (4), 341–361.

Vaganay, J., Baccou, P., Jouvencel, B., 2000. Homing by acoustic ranging to a single beacon. In: OCEANS 2000 MTS/IEEE Conference and Exhibition, vol. 2. IEEE, pp. 1457–1462.

Vallicrosa, G., Bosch, J., Palomeras, N., Ridao, P., Carreras, M., Gracias, N., 2016. Autonomous Homing and Docking for Auvs Using Range-only Localization and Light Beacons, vol. 49. IFAC-PapersOnLine, pp. 54–60 (23).

Vallicrosa, Guillem, Ridao, Pere, 2016. Sum of Gaussian single beacon range-only localization for auv homing. Annu. Rev. Contr. 42, 177–187.

Wang, Sen, Chen, Ling, Hu, Huosheng, Gu, Dongbing, 2013. Single beacon based localization of AUVs using moving Horizon estimation. In: Intelligent Robots and Systems (IROS), 2013 IEEE/RSJ International Conference on. IEEE, pp. 885–890.

Webster, Sarah E., Eustice, Ryan M., Singh, Hanumant, Whitcomb, Louis L., 2009. Preliminary deep water results in single-beacon one-way-travel-time acoustic navigation for underwater vehicles. In: Intelligent Robots and Systems, 2009. IROS 2009. IEEE/RSJ International Conference on. IEEE, pp. 2053–2060.

Yoerger, Dana R., Jakuba, Michael, Bradley, Albert M., Bingham, Brian, 2007. Techniques for deep sea near bottom survey using an autonomous underwater vehicle. Int. J. Robot Res. 26 (1), 41–54.

Zhang, Z., Nov 2000. A flexible new technique for camera calibration. IEEE Trans. Pattern Anal. Mach. Intell. ISSN: 0162-8828 22 (11), 1330–1334. https://doi.org/10.1109/34.888718.